

# Reversible vs Standard Hydrogen Electrode Scale in Interfacial Electrochemistry from a Theoretician's Atomistic Point of View

Axel Groß\*



Cite This: <https://doi.org/10.1021/acs.jpcc.2c02734>



Read Online

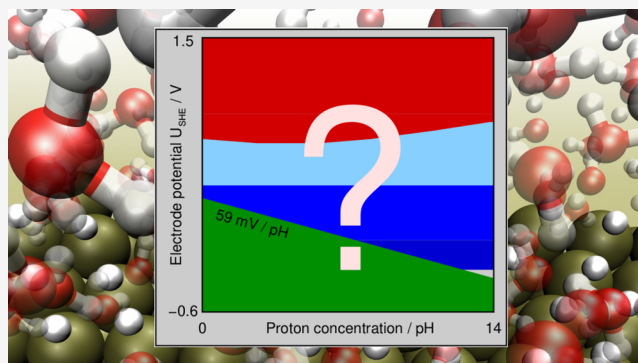
ACCESS |

Metrics & More

Article Recommendations

**ABSTRACT:** It is a general notion in interfacial electrochemistry that the stability of adsorbate phases that only contain hydrogen atoms should be independent of the pH value of the electrolyte on the scale of the reversible hydrogen electrode, whereas the stability of adsorbate phases that do not contain any hydrogen should be independent of the pH value on the scale of the standard hydrogen electrode. In this Perspective, it will be argued on the basis of a grand-canonical approach that such a Nernstian behavior can only be reproduced if the free energy of the adsorbate phase is independent of the electrochemical control parameters. In general, this should not be true, so that the Nernstian behavior should be the exception rather than the rule. Still, structural and chemical factors will be discussed that might lead to a Nernstian behavior.

This requires an analysis of the electrochemical electrolyte/electrode interface on the atomistic level. At the same time, this analysis also provides a guideline for the validity of grand-canonical simulations using the concept of the computational hydrogen electrode in which the dependence of the energy of adsorbate phases on pH and electrode potential is neglected.



## 1. INTRODUCTION

Electrochemical energy storage and conversion is of critical importance for our future sustainable, environmentally friendly energy supply.<sup>1,2</sup> Due to this importance, significant research and development efforts are undertaken worldwide in order to improve our understanding of electrochemical processes at electrolyte/electrode interfaces and to develop more efficient electrochemical devices such as electrocatalysts, fuel cells, and batteries. Electrochemistry as a research field can be traced back to the end of the 18th century with the experiments of Galvani and Volta.<sup>3</sup> Here I focus on interfacial electrochemistry, which is concerned with “structures and processes at the interface between an electronic conductor (the electrode) and an ionic conductor (the electrolyte) or at the interface between two electrolytes”.<sup>3</sup> In particular, I will consider structures at electrochemical electrolyte/electrode interfaces in thermodynamical equilibrium. At such interfaces, usually the existence of an electric double layer (EDL) is proposed based on the assumption that excess charges form on the two sides of the interfaces.<sup>3</sup>

In fact, the concepts to understand the structure of an electric double layer had been developed more than 100 years ago,<sup>4–7</sup> and in principle, our understanding of such interfaces is still influenced by these concepts, which are based to a large extent on a continuum description of electrochemical interfaces. Although there have been attempts to establish an atomistic view of electrochemistry,<sup>8,9</sup> electrochemistry still appears to be a

field whose perception and understanding is based on thermodynamical concepts. These thermodynamical concepts are the consequence of deep insights into the basic rules governing electrochemistry.<sup>3</sup> Still, thermodynamics is a field that deals with measurable macroscopic physical quantities, but a full understanding of the nature of these quantities requires a connection to microscopic properties via statistical mechanics. I will illustrate this using the dependence of adsorbate phases on the pH value and the electrode potential.

In electrochemistry, the concept of potentials is of central importance.<sup>10</sup> For a newcomer in electrochemistry, the subtleties between various different potential definitions might cause some confusion. Some potentials depend on position, such as the inner or Galvani potential,<sup>3</sup> and some are rather intensive properties such as the electrode potential. Both these potentials are measured in units of a voltage, but for example, the electrochemical potential, which also is an intensive property, is measured in units of an energy. It is also important to stress that structures and processes at electrochemical electrolyte/

**Received:** April 20, 2022

**Revised:** May 23, 2022

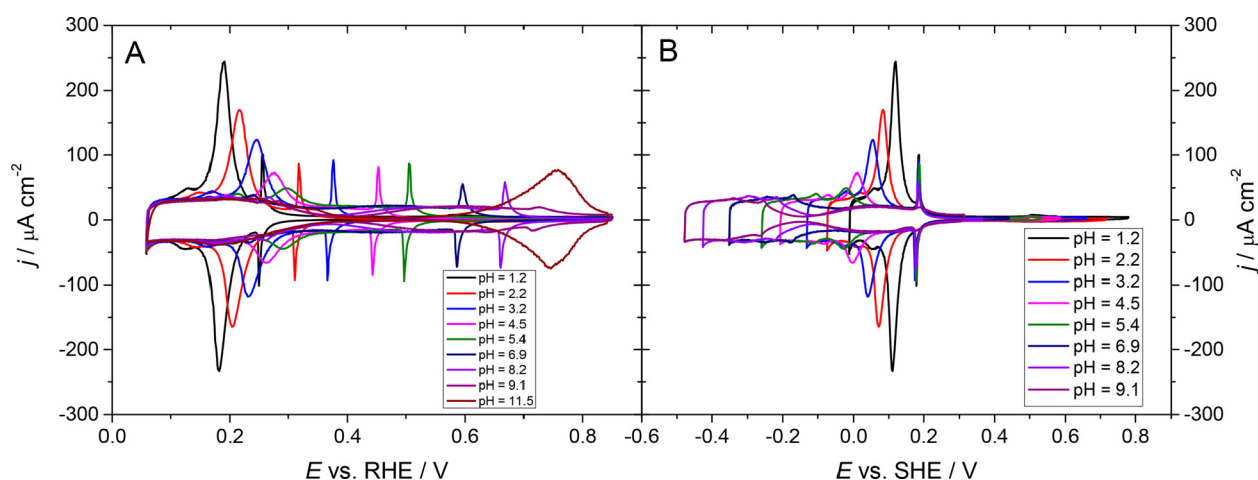


**Figure 1.** Cyclic voltammograms for Pt(111) in different solutions with pH values ranging from 1.2 to 11.5 in the presence of  $10^{-2}$  M KBr in the RHE scale (A) and in the SHE scale (B). Reprinted with permission from ref 20. Copyright 2018 American Chemical Society.

electrode interfaces are typically rather complex. Together with the wealth of electrochemical concepts, this sometimes leads to misconceptions (see, e.g., the “HOMO–LUMO misconception” about the electrochemical stability window of battery electrolytes<sup>11</sup>), which, on the other hand, turn electrochemistry into a very vivid field of scientific discussions.

In this Perspective, I will discuss the difference between electrode potentials measured with respect to the standard hydrogen electrode (SHE) and the reversible hydrogen electrode (RHE). In contrast to the SHE, electrode potentials vs RHE change with the pH value of the electrolyte.<sup>12</sup> As far as equilibrium structures of electrochemical electrolyte/electrode interfaces are concerned, I will particularly address the question what it means if the stability of an interface structure does not change as a function of the electrode potential vs RHE for different pH values. Admittedly, it appears to me as if there is some confusion about the interpretation of such findings in the literature, which baffled me for a long time. Typically, it is assumed that hydrogen evolution and oxidation at electrochemical interfaces should follow the Nernst equation. This means that they should be pH-independent on the RHE scale and exhibit a 59 mV shift for every unit of pH change at room temperature on the SHE scale.<sup>13–17</sup> In fact, any deviation from this behavior has been regarded as being “anomalous”. Such a Nernstian behavior is well-known from molecular electrochemistry<sup>18</sup> and apparently was simply transferred to interfacial electrochemistry. In those cases in which an anomalous behavior has been observed, a broad range of explanations for this phenomenon has been presented. On the one hand, such an anomalous shift has been related to a pH-dependent hydrogen binding energy,<sup>19</sup> but on the other hand, it has been argued that the hydrogen binding energy should be an intrinsic material property and thus not depend on experimental conditions such as the pH value so that other explanations need to be invoked.<sup>17</sup> Conversely, it is assumed that adsorbate phases at electrified interfaces that do not contain any hydrogen should not be pH-dependent on the SHE scale.

Here, I will discuss the differences between the SHE and the RHE in interfacial electrochemistry from an atomistic theoretical point of view based on a grand-canonical formalism. I will argue that in principle the stability of any adsorbate structure should be dependent on pH and electrode potential, no matter what specific electrode potential has been chosen.

This means that hydrogen equilibrium interface structure should be pH-dependent, even on the RHE scale, and structures not containing any hydrogen should be pH-dependent on the SHE scale. Thus, the anomalous behavior should be the rule rather than the exception. Still, I will also give arguments why often these shifts should be rather small.

## 2. MOTIVATION

The study of processes at electrochemical interfaces involving hydrogen adsorption and desorption is of considerable interest, both from a fundamental and from a technological point of view due to its importance in electrochemical energy conversion. In fact, whenever aqueous electrolytes are involved, then naturally hydrogen adsorption can occur due to the fact that there is always a nonzero concentration of protons in the electrolyte. As an illustration of such a system, I have picked a recent experimental study of bromide adsorption on Pt(111),<sup>20</sup> which had also been studied theoretically by first-principles calculations.<sup>21,22</sup> At electrochemical interfaces between an aqueous electrolyte and in particular metal electrodes, at low electrode potentials at which the electrode is assumed to be more negatively charged, cation adsorption is more favorable (here proton adsorption), whereas at higher potentials at which the electrode is more positively charged, anions such as halides adsorb preferentially. In fact, experimentally a competitive adsorption of hydrogen and halides on Pt(111) has been observed at low pH values,<sup>23,24</sup> i.e., upon increasing the electrode potential adsorbed hydrogen is replaced by chloride or bromide, respectively, which has also been confirmed in first-principles calculations.<sup>21,22</sup>

Figure 1 shows cyclic voltammograms of Pt(111) in the presence of  $10^{-2}$  M KBr for different pH values both on the RHE (panel A) and the SHE (panel B) scale. First of all it can be seen that the voltammograms are rather symmetric, indicating that the peaks correspond to reversible processes. There are two prominent peaks in each scan. First, there is a large broad peak at 0.18 V vs RHE at pH = 1.2 which shifts to higher voltages for increasing pH values and splits to a certain extent. This peak is associated with hydrogen adsorption/desorption and bromide adsorption/desorption,<sup>20</sup> which strongly overlap at low potentials indicating the competitive nature of hydrogen and bromide adsorption.<sup>24</sup> Whereas this peak shifts to higher voltages with increasing pH vs RHE, it shifts to lower voltages vs

SHE, thus showing a non-Nernstian behavior. There is another sharp peak at 0.2 V vs SHE which stays constant on the SHE scale as a function of pH. It is attributed to a Pt(111)(4×4)-7Br to Pt(111)(3×3)-4Br transition which does not involve any hydrogen and therefore should be pH-independent on the SHE scale.<sup>20</sup>

### 3. THEORETICAL METHODOLOGY

As discussed in the previous section, the peaks in the cyclic voltammograms shown in Figure 1 are associated with reversible changes in the structure and coverage of the electrode surface. The stable equilibrium structures of electrochemical electrolyte/electrode interfaces can be conveniently determined using grand-canonical schemes as a function of the electrochemical environment.<sup>25,26</sup> This environment is characterized by the electrode potential  $U$  and the activities  $a_i$  of the species  $i$  solvated in the electrolyte which for an ideal solution corresponds to their concentration or for protons can be expressed through the pH value. In order to determine the stable structures, it is helpful to subdivide the electrolyte/electrode interface into three regions as illustrated in the lower part of Figure 2: bulk electrode, bulk

for the adsorption of  $N_i$  particles of species  $i$  in the interface region is negative.  $G^{\text{interf}}(T, U, a_i, N_i)$  is the free energy of the interface region with  $N_i$  adsorbates of species  $i$  present in the interface region and  $\tilde{\mu}_i(T, U, a_i)$  the electrochemical potential of species  $i$ . Now it is important to realize that it is not the free energy of adsorption per particle of species  $i$  that determines the thermodynamically stable interface structure but rather the free energy of adsorption per surface area  $A_S$ :<sup>26</sup>

$$\Delta\gamma(T, U, a_i, N_i) = \Delta G^{\text{ads}}(T, U, a_i, N_i)/A_S \quad (2)$$

From now on we implicitly assume that we have a periodic adsorbate structure and that  $A_S$  is the surface area of the unit cell with  $N_i$  adsorbed species.

One critical problem in calculating the adsorption free energy  $\Delta G^{\text{ads}}$  according to eq 1 is due to the fact that the determination of the electrochemical potential  $\tilde{\mu}_i(T, U, a_i)$  typically requires the evaluation of solvation energies which is computationally rather demanding.<sup>28</sup> However, this evaluation can be avoided by relating the electrochemical potential of the solvated species to the chemical potential of corresponding gas-phase species via the redox potential which is the basis of the concept of the computational hydrogen electrode (CHE) proposed by Nørskov et al.<sup>25,27</sup> For hydrogen adsorption, this means that the electrochemical potential of hydrogen can be expressed as

$$\begin{aligned} \tilde{\mu}_{\text{H}} &= \tilde{\mu}_{\text{H}^+(\text{aq})} + \tilde{\mu}_{\text{e}^-} = \frac{1}{2}\mu_{\text{H}_2(\text{g})} - eU_{\text{SHE}} - k_{\text{B}}T \ln(10) \text{ pH} \\ &= \frac{1}{2}\mu_{\text{H}_2(\text{g})} - eU_{\text{RHE}} \end{aligned} \quad (3)$$

This equation requires some clarification. First of all I have written the electrochemical potential of hydrogen as the sum of the electrochemical potentials of the proton and the electron. Note that, in eq 1, the energy for the adsorption of  $N_i$  particles of species  $i$  is considered. Note furthermore that in thermal equilibrium electrochemical electrolyte/electrode interface have to be overall charge neutral because otherwise there would be a net electric field which would attract or repel charged particles with respect to the interface.<sup>29</sup> So the presence of a proton close to the interface requires the presence of a corresponding countercharge, which usually means for metallic electrodes that there is an additional electron at the Fermi level in the electrode. Hence the adsorption of a proton at this electrified interface leads effectively to the adsorption of a hydrogen atom on the electrode, and therefore, we have to take the electrochemical potential  $\tilde{\mu}_{\text{H}^+(\text{aq})} + \tilde{\mu}_{\text{e}^-}$  of a solvated hydrogen atom as a reference.

Furthermore, eq 3 also demonstrates that it does not matter whether the electrode potential is given on the SHE or the RHE scale (or any other potential scale), the electrochemical potential has to be independent of the choice of the reference for the electrode potential. Hence the CHE is neither a “RHE concept” nor a “SHE concept”; it is just a grand-canonical concept. Consequently, also the adsorption energy cannot not depend on the particular choice of the electrode potential scale. Hence the free energy of hydrogen adsorption per surface area at electrochemical interfaces as a function of the electrochemical control parameters can for example be expressed as

$$\begin{aligned} \Delta\gamma_{\text{H}}(T, U, \text{pH}, N_{\text{H}}) &= \frac{N_{\text{H}}}{A_S} (\Delta G_{\text{H}}^{\text{ads}}(T, U, \text{pH}) + eU_{\text{SHE}} \\ &\quad + k_{\text{B}}T \ln(10) \text{ pH}) \end{aligned} \quad (4)$$

where

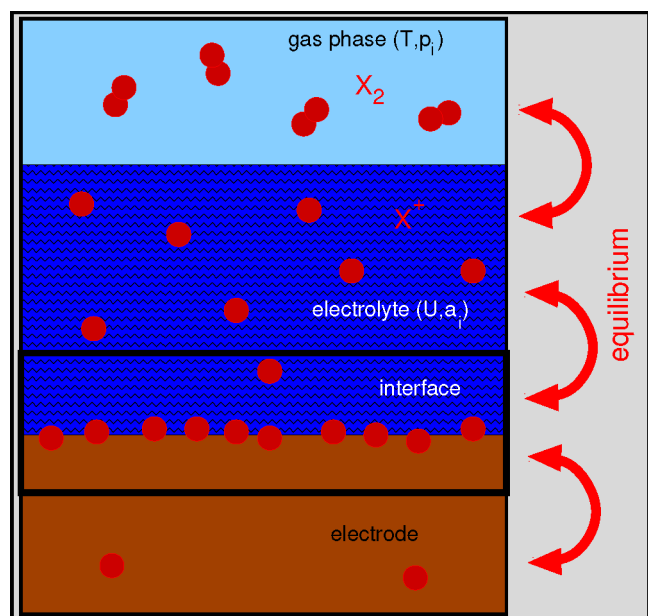


**Figure 2.** Illustration of a grand-canonical scheme to determine the equilibrium structure of electrode–electrolyte interfaces. The inclusion of the gas phase is the basis for the concept of the computational hydrogen electrode (CHE).<sup>25,27</sup> The interface region is given by the area in the box. Adapted from ref 26 and reprinted with permission from ref 26. Copyright 2021 Elsevier.

electrolyte, and the interface region. Furthermore, we assume that there is thermal equilibrium throughout the system which means that the (electro-)chemical potentials of the species present in the systems are constant throughout the whole system.

Now consider a clean interface without any adsorbates. A species  $i$  present in the electrolyte will adsorb at the electrochemical interface if the free energy difference

$$\begin{aligned} \Delta G^{\text{ads}}(T, U, a_i, N_i) &= G^{\text{interf}}(T, U, a_i, N_i) \\ &\quad - G^{\text{interf}}(T, U, a_i, 0) - N_i \tilde{\mu}_i(T, U, a_i) \end{aligned} \quad (1)$$

$$\Delta G_{\text{H}}^{\text{ads}}(T, U, \text{pH}) = \frac{1}{N_{\text{H}}}(G_{\text{A}_s}^{\text{interf}}(T, U, \text{pH}, N_{\text{H}}) - G_{\text{A}_s}^{\text{interf}}(T, U, \text{pH}, 0)) - \frac{1}{2}\mu_{\text{H}_2(\text{g})} \quad (5)$$

corresponds to the free adsorption energy per hydrogen atom in the structure with  $N_{\text{H}}$  adsorbed hydrogen atoms per surface area  $A_s$  with respect to the hydrogen molecule in the gas phase. This concept can also be used for the adsorption of, e.g., halides  $\text{A}^-$  with  $\text{A} = \text{F}, \text{Cl}, \text{Br}, \text{I}$ , where typically the redox couple is given by  $\frac{1}{2}\text{A}_2 + \text{e}^- \rightleftharpoons \text{A}^-$  yielding an electrochemical potential of<sup>30,31</sup>

$$\begin{aligned} \tilde{\mu}(\text{A}^-(\text{aq})) - \tilde{\mu}(\text{e}^-) \\ = \frac{1}{2}\mu(\text{A}_2(\text{g})) + e(U_{\text{SHE}} - U^0) + k_{\text{B}}T \ln a_{\text{A}^-} \end{aligned} \quad (6)$$

where  $U^0$  is the reduction potential of the halide vs  $U_{\text{SHE}}$  and  $a_{\text{A}^-}$  its activity coefficient. Furthermore, also any mixed adsorbate phase can be addressed using this approach.

#### 4. DISCUSSION

In the previous section, I described the grand-canonical approach to determine the thermodynamically stable adsorbate phases at electrochemical electrolyte/electrode interfaces. In order to avoid the evaluation of solvation energies of solvated species, the concept of the computational hydrogen electrode<sup>25,27</sup> has been employed. It is important to note that up to here all expressions are exact, as far as the description of structures in thermodynamic equilibrium is concerned. However, the evaluation of the corresponding expressions requires the determination of free energies which is typically numerically rather demanding as it necessitates performing, e.g., thermodynamic integration schemes.

Hence typically in the application of the CHE, the free energy difference appearing in eq 5 is replaced according to

$$\begin{aligned} G_{\text{A}_s}^{\text{interf}}(T, U, \text{pH}, N_{\text{H}}) - G_{\text{A}_s}^{\text{interf}}(T, U, \text{pH}, 0) \\ \approx E_{\text{A}_s}^{\text{interf}}(N_{\text{H}}) - E_{\text{A}_s}^{\text{interf}}(0) \end{aligned} \quad (7)$$

which means that the difference in the free energies is replaced by the difference in total energies, and in the evaluation of the total energies, the electrochemical control parameters are neglected; i.e., the interface energies are assumed to be independent of the electrode potential and proton concentration. Often the electrochemical environment is entirely neglected; i.e., the total energies are calculated at the vacuum/electrode interface instead of the electrolyte/electrode interface.<sup>21,31</sup> Thus, for example, the capacitive charging of the diffuse double layer is not captured at all which has been identified as a critical factor in interfacial electrochemistry.<sup>32</sup> Still it is important to emphasize that this is not an approximation that is inherent to the CHE, as is often assumed, but rather a typical approximation applied when employing the in principle exact concept of the CHE.<sup>26</sup>

I will now discuss a typical example presented in Figure 3 where the approximations just mentioned have all been invoked. This figure displays a Pourbaix diagram, i.e., a phase diagram as a function of pH and the electrode potential, calculated within the concept of the CHE.<sup>22</sup> This Pourbaix diagram addresses exactly the same system as covered in Figure 1, namely the coadsorption of hydrogen and bromide on Pt(111) in the presence of an aqueous electrolyte. In these calculations, a fixed bromide concentration corresponding to an activity of  $a = 0.1$  has been

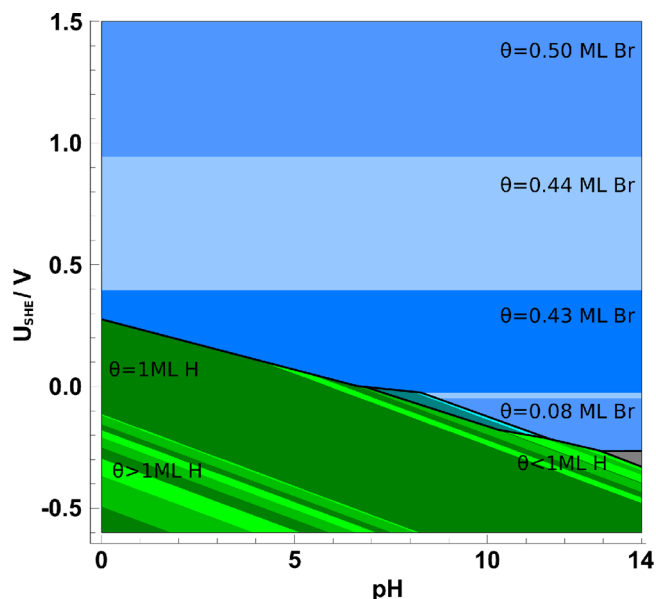


**Figure 3.** Calculated Pourbaix diagram, i.e., a map of the stable phases of coadsorbed bromine and hydrogen on Pt(111) as a function of pH and electrode potential for a fixed bromide concentration corresponding to an activity of  $a = 0.1$ . Greenish colors denote a pure hydrogen phase, while bluish colors denote a pure bromine phase. In between the hydrogen and bromine phases, there is a thin region where a coadsorbate structure with both species is stable. The gray area corresponds to a region where the clean, uncovered electrode is stable. Reprinted with permission from ref 22. Copyright 2016 American Chemical Society.

assumed that might be somewhat larger than the concentration of  $10^{-2}$  M KBr used in the experiments.<sup>20</sup>

The greenish phases in Figure 3 correspond to pure hydrogen adsorbate phases and the bluish ones to pure bromide adsorbate phases. Furthermore, there is a small pocket of mixed hydrogen-bromide adsorption phases at intermediate pH values. However, at low pH values, the DFT calculations nicely reproduce the competitive adsorption of hydrogen and bromide observed in the experiment;<sup>20,24</sup> i.e., the adsorbed hydrogen is replaced by adsorbed bromide upon increasing the electrode potential.

Replacing the free energies in eq 5 by total energies according to eq 7 means that the dependence of the stability of the pure hydrogen adsorbate phase on pH only enters through the term  $k_{\text{B}}T \ln(10)$  pH appearing in the electrochemical potential of the solvated protons. Also the electrode potential does not affect the difference in the interface energies. And sure enough, the boundaries between the pure hydrogen adsorption phases all exhibit a slope of 59 mV/pH; i.e., they exhibit a perfect Nernstian behavior.

Now this Nernstian behavior has not been observed in the experiment<sup>20</sup> with respect to the hydrogen adsorption/desorption and bromide adsorption/desorption or, instead, the competitive replacement of adsorbed hydrogen by bromide and *vice versa*. Interestingly, the calculated phase boundary between the purely hydrogen-adsorbate phases and the purely bromide adsorption phase at pH values below 7 in Figure 3 exhibits a slope that is smaller than 59 mV/pH. Upon changing pH from 1.2 to 5.4, the corresponding peak in the CV shown in Figure 1B shifts by roughly 120 mV, whereas the corresponding shift in Figure 3 is about 140 mV. Thus, a seemingly non-Nernstian behavior is in fact reproduced in calculations in which the free energy difference  $\Delta G_{\text{H}}^{\text{ads}}(T, U, \text{pH})$  expressed in eq 5 does

not depend on pH and electrode potential  $U$ . The solution of this surprising result rests in the competitive nature of hydrogen and bromide adsorption at this phase boundary. Neglecting the pH and  $U$  dependence of  $\Delta G_{\text{H}}^{\text{ads}}(T, U, \text{pH})$  leads to purely Nernstian behavior of the stability of the hydrogen adsorbate phases, but at the same time, it makes the stability of the bromide phases pH-independent. The competition between a phase that depends on pH and a phase that does not depend on pH makes the phase transition pH-dependent with a slope that is lower than 59 mV/pH which depends on the coverage of both phases.<sup>21</sup>

Another interesting feature of the cyclic voltammograms shown in Figure 1 is the observation that the peak related to the change in the bromide structure does not depend on pH on the SHE scale. Interestingly enough, in the calculations presented in Figure 3, also a structural change in the bromide adlayer from a  $(\sqrt{7} \times \sqrt{7} R19.1^\circ) - 3\text{Br}$  to a  $(3 \times 3) - 4\text{Br}$  structure has been found. This is not exactly the same transition as the one attributed to the corresponding peak by Mello et al.<sup>20</sup> where a  $(4 \times 4) - 7\text{Br}$  has been assumed at lower electrode potentials, however, the coverage change upon this transition is almost the same. It is also gratifying to see that the calculations at least qualitatively reproduce the experimental observation<sup>20</sup> that toward alkaline conditions the bromide adsorption peak separates from the hydrogen desorption peak. Note, however, that OH adsorption is not considered in the calculations which might replace bromide adsorption under very alkaline conditions.<sup>20</sup>

With respect to the fact that this transition between two different bromide adsorption phases is pH independent, both theory and experiment thus agree. But again, there is no fundamental reason to presuppose that the free energy difference  $\Delta G^{\text{ads}}(T, U, \text{pH})$  with regard to bromide adsorption should be independent of any changes in pH. For example, recently a pH dependence has been found in the calculated activity of the oxygen evolution reaction  $\beta\text{-NiOOH}(0001)$  on the RHE scale,<sup>33</sup> in agreement with the experiment.<sup>34</sup> This pH dependence has been mediated by the explicit consideration of a pH-dependent electric double layer structure in the calculations. Note, furthermore, that in experiments changing the pH value typically also requires to use electrolytes with different counterions, in particular if a wide range of pH values from acidic to alkaline conditions is scanned.<sup>20</sup> Again, the particular choice of the counterions can significantly modify the properties of the electric double layer, causing, e.g., an apparent pH dependence of hydrogen adsorption on a stepped Pt electrode on the RHE scale<sup>35</sup> or a strong dependence of the Pt(111) double-layer capacitance on the particular choice of the electrolyte.<sup>36</sup>

However, there are good arguments why this free adsorption energy in particular of small ions such as protons or halides at electrochemical interfaces between an aqueous electrolyte and a metal electrode should be rather independent of pH and electrode potential. Note that, at pH = 0, there is one proton per 55 water molecules. Already at pH = 2, there are 5500 water molecules per one proton. Although the proton concentration close to the electrochemical interface might be larger than in the bulk electrolyte, it is rather unlikely that such a minute concentration of protons should change the hydrogen adsorption energies. Furthermore, electric field effects directly at metal electrodes are very effectively shielded due to the fact that an electric field cannot penetrate into an ideal conductor.<sup>37</sup> This provides an explanation why changes in the electrode

potential might hardly affect the adsorption energies of small atomic adsorbates such as hydrogen and halides. And, last but not least, even the presence of water hardly modifies adsorption energies of atoms at metal surfaces due to the relatively weak interaction of water with metal surfaces and the comparable large distance of the water molecules from the surface.<sup>25,38,39</sup>

One can now turn the argumentation around with respect to the validity of the approximations often entering applications of the concept of the computational hydrogen electrode. Recent theoretical studies have correctly emphasized that it is important to take the electrochemical environment adequately into account in the modeling of electrolyte/electrode interfaces.<sup>40–43</sup> However, for those electrochemical interfacial systems in which hydrogen adsorbate phases exhibit a Nernstian behavior or in which the stability of non-hydrogen adsorption phases does not depend on pH, it can in principle safely be assumed that the free energy difference  $\Delta G_{\text{H}}^{\text{ads}}(T, U, \text{pH})$  does not depend on the electrochemical control parameters, so that this difference can be replaced by the difference in the respective total energies. For example, the fact that the peak in the cyclic voltammograms related to the change in the bromide structure in Figure 3 does not depend on pH on the SHE scale, in spite of the fact that different electrolytes have been used at low and high pH values, indicates that the presence of the electrolyte either hardly influences the stability of the bromide adsorbate phases or just leads to a constant shift independent of the particular structure of the EDL. Hence the presence of the EDL can be safely neglected in the evaluation of the relative stability of the bromide adsorption phases. This also provides an explanation why the typical approximation applied when doing calculations of electrochemical interfaces using the concept of the computational hydrogen electrode, namely to neglect the influence of electrode potential and pH when calculating the energy of the adsorbate phases, has often yielded results that agree rather nicely with the experiment.<sup>29,44–49</sup>

To wrap up this discussion of the difference between the reversible and the standard hydrogen electrode, I will present another example of a Pourbaix diagram produced using the concept of the CHE neglecting the pH and electrode potential dependence in the adsorption energy with respect to the free  $\text{H}_2$  molecule. This example is concerned with the adsorption of sulfate and hydrogen on Pt(111) and Au(111).<sup>44</sup> Note that similar results for Au(111) as presented in ref.<sup>44</sup> have also been found in a recent joint experimental-theoretical work.<sup>50</sup> Here, however, I will concentrate on sulfate adsorption on Pt(111). On this surface, sulfate adsorbs at potentials of about 0.5 V in a row-like  $\sqrt{3} \times \sqrt{7}$  structure<sup>51</sup> whereas the corresponding structure appears on Au(111) at potentials of about 1 V.<sup>52</sup> Still, DFT calculations neglecting the explicit presence of water molecules on these surfaces fail to reproduce the presence of any stable row-like sulfate structures at the experimentally observed conditions.<sup>44</sup> Also the inclusion of water within an implicit solvent model<sup>53</sup> could not heal this discrepancy between experiment and theory.

However, using a combination of the implicit solvent model with explicitly considered water molecules, a very satisfactory agreement with the experiment has been obtained. This is demonstrated in Figure 4 where a Pourbaix diagram for the coadsorption of sulfate and hydrogen on Pt(111) is shown. At low electrode potentials, Pt(111) is hydrogen-covered, and at about 0.4 V the so-called double layer region starts, in which Pt(111) is not covered by any adsorbate, followed by the onset of sulfate adsorption. The structure of the stable row-like

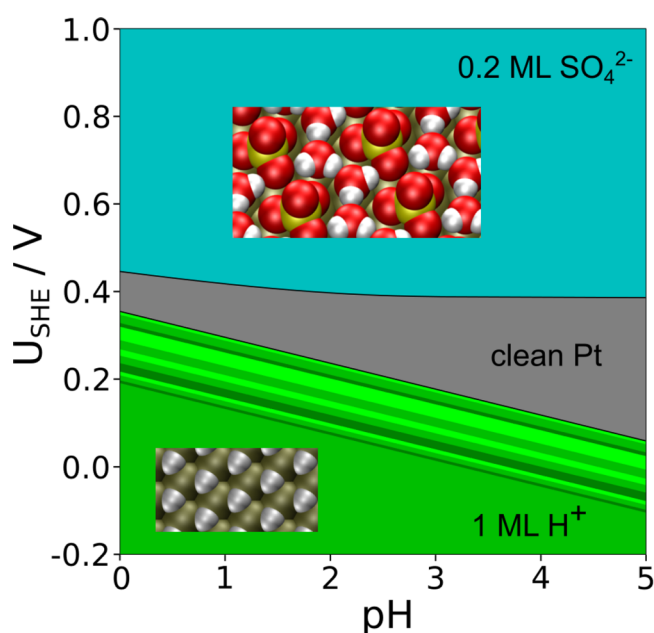


**Figure 4.** Calculated Pourbaix diagram showing the stable phases of coadsorbed sulfate and hydrogen on Pt(111) as a function of pH and electrode potential.<sup>44</sup> The sulfate concentration corresponds to an activity of 0.1. Reprinted with permission from ref 26. Copyright 2021 Elsevier.

$\sqrt{3} \times \sqrt{7}$  sulfate phase is illustrated in the inset of Figure 4. This sulfate row-like structure becomes strongly stabilized by the presence of two explicit water molecules per sulfate anion linking the sulfate rows. These water molecules are strongly bound with a binding energy that is much higher than the water cohesive energy<sup>44,50</sup> so that they become an integral immobile element of the sulfate adsorbate structure.

This example shows that the presence of water can indeed have a significant influence on the stability of adsorbate phases at interfaces between aqueous electrolytes and electrodes, even without the explicit consideration of pH and the electrode potential. However, in the case of sulfate adsorption on Pt(111) and Au(111) the combination of frozen water rows together with an implicit solvent was sufficient to yield a qualitative and semiquantitative agreement with experiment.<sup>44,50</sup> In general, the liquid nature of water has to be appropriately taken into account in order to faithfully model water/electrode interfaces. Unfortunately, considering the explicit presence of water molecules requires one to perform time-consuming averages, for example, based on *ab initio* molecular dynamics (AIMD) simulations.<sup>54–57</sup> As a computationally attractive alternative, the explicit description of water molecules might be replaced by using implicit solvent models in which the solvent is described by a dielectric continuum just characterized by its dielectric constant.<sup>41,42</sup> Unfortunately, benchmark calculations found substantial deviations between AIMD and implicit solvent approaches,<sup>58</sup> as far as the influence of solvation on adsorption energies is concerned. Hence it appears fair to say that further work is required to obtain a reliable and at the same time computationally attractive approach to model interfaces between aqueous electrolytes and electrodes.

Note that the calculations presented in Figure 4 also reproduce the experimentally observed displacement of sulfate adsorption to higher potentials for decreasing pH, in particular for  $\text{pH} \geq 2$ ,<sup>59</sup> resulting in a curved phase boundary between

clean Pt and the sulfate adsorption phase. This is interesting as the pH value does not directly enter the electrochemical potential of sulfate<sup>44</sup> under equilibrium conditions. However, there is an acid/base equilibrium between protons, sulfate and bisulfate anions  $\text{HSO}_4^- \rightleftharpoons \text{SO}_4^{2-} + \text{H}^+$ . Furthermore, for the calculation of the Pourbaix diagrams, the total concentration of anions  $c_i$  in the electrolyte has to be kept fixed which makes the molar fraction  $x_i$  of  $\text{SO}_4^{2-}$  pH-dependent according to<sup>44</sup>

$$x_{\text{SO}_4^{2-}} = \frac{1}{1 + 10^{-\text{pH}}/10^{-\text{pK}_a}} \quad (8)$$

Thus, it is the molar fraction of sulfate through which the onset of the sulfate adsorption phase becomes pH-dependent.

It is important to recall that the two Pourbaix diagrams just discussed were determined using the approximation that the adsorption energies of the considered adsorbate phases do not depend on electrode potential and proton concentration. Thus, the dependence of the stable phases on electrode potential and pH entirely stems from the corresponding dependence of the electrochemical potential of the species in solution. And, as already discussed above, this is exactly the assumption the Nernstian view on the stability of adsorbate phases is based on, as it only takes the thermodynamics of the bulk electrolyte into account. This is also the reason these calculations yield a stability of pure hydrogen adsorbate phases that changes by 59 mV/pH whereas the stability of adsorbate phases that contain no hydrogen are independent of pH. The sulfate example shown in Figure 4 demonstrates that only adsorbate phases that involve species consisting of hydrogen and other elements can exhibit a nontrivial dependence on electrode potential and pH. This is in fact also illustrated for the small pocket of mixed H–Br adsorbate phases in Figure 3. Overall, this means that those interfacial systems, for which grand-canonical simulations employing the approximation in eq 7 are able to faithfully reproduce the experimentally observed existence of stable adsorbate phases, are dominated by a Nernstian behavior; i.e., the dependence of the stable adsorbate phases on the electrochemical control parameters pH and electrode potential are governed by the properties of the bulk electrolyte. Any deviation from this behavior requires a careful analysis of the stability determining factors of the explicit adsorbate phases on an atomistic level.

## 5. CONCLUSIONS

In this Perspective, the stability of adsorbate phases at electrochemical electrolyte/electrode interfaces has been addressed from a theoretical atomistic point of view based on a grand-canonical approach. As for any adsorbate phase, its thermodynamic stability is governed both by the reservoir the adsorbate originates from and by the free energy of the adsorbate structure. Neglecting the dependence of the free energy of the adsorbate structure on pH and electrode potential leads to a Nernstian behavior; i.e., the stability of adsorbate phases that only contain hydrogen atoms becomes independent of the pH value of the electrolyte on the scale of the reversible hydrogen electrode, whereas the stability of adsorbate phases that do not contain any hydrogen becomes independent of the pH value on the scale of the standard hydrogen electrode. Indeed, there are good arguments on the atomistic level, in particular for the case of small atomic adsorbates on metal electrodes, that make these assumptions underlying the Nernstian behavior reasonable. These arguments also explain the success of grand-canonical simulations of adsorbate phases using the concept of the

computational hydrogen electrode in which the influence of the electrochemical control parameters on the energy of the adsorbate phases are neglected. In general, however, this approximation should not be valid. Changing electrode potential and/or pH alters the structure of the electric double layer at the interface, which will also modify the local electric field close to the electrode. Hence there is no reason to assume that the free energy of electrified interfaces should be independent of electrode potential and pH. Therefore, the “normal” Nernstian behavior should be the exception rather than the rule. Consequently, the study of any adsorbate structure at electrochemical interfaces requires a careful analysis of the factors influencing its stability on the atomistic level.

## AUTHOR INFORMATION

### Corresponding Author

Axel Groß – Institute of Theoretical Chemistry, Ulm University, 89069 Ulm, Germany; Electrochemical Energy Storage, Helmholtz Institute Ulm (HIU), 89081 Ulm, Germany;  
orcid.org/0000-0003-4037-7331; Email: axel.gross@uni-ulm.de

Complete contact information is available at:  
<https://pubs.acs.org/10.1021/acs.jpcc.2c02734>

### Notes

The author declares no competing financial interest.

### Biography



Elvira Eberhardt

Axel Groß obtained his Diploma in Physics from the University of Göttingen in 1990 and his Ph.D. in 1993 in Theoretical Physics at the Technical University of Munich. After 5 years as a staff scientist in the Theory Department of the Fritz-Haber-Institute of the Max-Planck-Society in Berlin, he became Associate Professor in Theoretical Physics/Surface Physics at the Technical University of Munich. In 2004, he was appointed as a Full Professor in Theoretical Chemistry at Ulm University; furthermore, in 2011, he became PI at Helmholtz Institute Ulm (HIU) Electrochemical Energy Storage. His research interests focus on the first-principles modeling of atomistic structures and processes at surfaces and at solid–gas and electrochemical electrode–electrolyte interfaces in electrochemical energy conversion and storage, reactions in heterogeneous catalysis and electrocatalysis, and materials modeling related to properties of batteries.

## ACKNOWLEDGMENTS

This work contributes to the research performed at CELEST (Center for Electrochemical Energy Storage Ulm-Karlsruhe). Support by the German Research Foundation (DFG) through

Contract GR 1503/39-1, the POLiS Cluster of Excellence, Project ID 390874152, and the Dr. Barbara Mez-Starck Foundation and discussions with Wolfgang Schmickler, Jürgen Behm, and Marc Koper are gratefully acknowledged.

## REFERENCES

- (1) Schlögl, R. The Role of Chemistry in the Energy Challenge. *ChemSusChem* **2010**, *3*, 209–222.
- (2) Abbas, Q.; Mirzaei, M.; Hunt, M. R.; Hall, P.; Raza, R. Current State and Future Prospects for Electrochemical Energy Storage and Conversion Systems. *Energies* **2020**, *13*, 5847.
- (3) Schmickler, W.; Santos, E. *Interfacial Electrochemistry*, 2nd ed.; Springer: Berlin, 2010.
- (4) Helmholtz, H. Studien über elektrische Grenzschichten. *Ann. Phys.* **1879**, *243*, 337–382.
- (5) Gouy, L. G. Sur la constitution de la charge électrique à la surface d'un électrolyte. *J. Phys. Theor. Appl.* **1910**, *9*, 457.
- (6) Chapman, D. L. A contribution to the theory of electrocapillarity. *Philos. Mag. Series 6* **1913**, *25*, 475–481.
- (7) Stern, O. Zur Theorie der Elektrolytischen Doppelschicht. *Z. Elektrochem. Angew. Phys. Chem.* **1924**, *30*, 508–516.
- (8) Kolb, D. M. An atomistic view of electrochemistry. *Surf. Sci.* **2002**, *500*, 722.
- (9) Magnussen, O. M.; Groß, A. Toward an Atomic-Scale Understanding of Electrochemical Interface Structure and Dynamics. *J. Am. Chem. Soc.* **2019**, *141*, 4777–4790.
- (10) Trasatti, S. The absolute electrode potential: an explanatory note. *Pure Appl. Chem.* **1986**, *58*, 955–966.
- (11) Peljo, P.; Girault, H. H. Electrochemical potential window of battery electrolytes: the HOMO–LUMO misconception. *Energy Environ. Sci.* **2018**, *11*, 2306–2309.
- (12) Jerkiewicz, G. Standard and Reversible Hydrogen Electrodes: Theory, Design, Operation, and Applications. *ACS Catal.* **2020**, *10*, 8409–8417.
- (13) Gisbert, R.; Garcia, G.; Koper, M. T. Adsorption of phosphate species on poly-oriented Pt and Pt(111) electrodes over a wide range of pH. *Electrochim. Acta* **2010**, *55*, 7961–7968.
- (14) van der Niet, M. J.; Garcia-Araez, N.; Hernandez, J.; Feliu, J. M.; Koper, M. T. Water dissociation on well-defined platinum surfaces: The electrochemical perspective. *Catal. Today* **2013**, *202*, 105–113.
- (15) Schwarz, K.; Xu, B.; Yan, Y.; Sundaraman, R. Partial oxidation of step-bound water leads to anomalous pH effects on metal electrode step-edges. *Phys. Chem. Chem. Phys.* **2016**, *18*, 16216–16223.
- (16) Yang, X.; Nash, J.; Oliveira, N.; Yan, Y.; Xu, B. Understanding the pH Dependence of Underpotential Deposited Hydrogen on Platinum. *Angew. Chem., Int. Ed.* **2019**, *58*, 17718–17723.
- (17) Rebellor, L.; Intikhab, S.; Oliveira, N. J.; Yan, Y.; Xu, B.; McCrum, I. T.; Snyder, J. D.; Tang, M. H. Beyond Adsorption” Descriptors in Hydrogen Electrocatalysis. *ACS Catal.* **2020**, *10*, 14747–14762.
- (18) Elgrishi, N.; Rountree, K. J.; McCarthy, B. D.; Rountree, E. S.; Eisenhart, T. T.; Dempsey, J. L. A Practical Beginner's Guide to Cyclic Voltammetry. *J. Chem. Educ.* **2018**, *95*, 197–206.
- (19) Durst, J.; Siebel, A.; Simon, C.; Hasché, F.; Herranz, J.; Gasteiger, H. A. New insights into the electrochemical hydrogen oxidation and evolution reaction mechanism. *Energy Environ. Sci.* **2014**, *7*, 2255–2260.
- (20) Mello, G. A. B.; Briega-Martos, V.; Climent, V.; Feliu, J. M. Bromide Adsorption on Pt(111) over a Wide Range of pH: Cyclic Voltammetry and CO Displacement Experiments. *J. Phys. Chem. C* **2018**, *122*, 18562–18569.
- (21) Gossenberger, F.; Roman, T.; Groß, A. Hydrogen and halide co-adsorption on Pt(111) in an electrochemical environment: a computational perspective. *Electrochim. Acta* **2016**, *216*, 152–159.
- (22) Lin, X.; Gossenberger, F.; Groß, A. Ionic Adsorbate Structures on Metal Electrodes Calculated from First-Principles. *Ind. Eng. Chem. Res.* **2016**, *55*, 11107–11113.

- (23) Garcia-Araez, N.; Climent, V.; Herrero, E.; Feliu, J.; Lipkowski, J. Thermodynamic studies of chloride adsorption at the Pt(111) electrode surface from 0.1 M HClO<sub>4</sub> solution. *J. Electroanal. Chem.* **2005**, *576*, 33–41.
- (24) Garcia-Araez, N.; Climent, V.; Herrero, E.; Feliu, J.; Lipkowski, J. Thermodynamic studies of bromide adsorption at the Pt(111) electrode surface perchloric acid solutions: Comparison with other anions. *J. Electroanal. Chem.* **2006**, *591*, 149–158.
- (25) Nørskov, J. K.; Rossmeisl, J.; Logadottir, A.; Lindqvist, L.; Kitchin, J. R.; Bligaard, T.; Jónsson, H. Origin of the Overpotential for Oxygen Reduction at a Fuel-Cell Cathode. *J. Phys. Chem. B* **2004**, *108*, 17886–17892.
- (26) Groß, A. Grand-canonical approaches to understand structures and processes at electrochemical interfaces from an atomistic perspective. *Curr. Opin. Electrochem.* **2021**, *27*, 100684.
- (27) Peterson, A. A.; Abild-Pedersen, F.; Studt, F.; Rossmeisl, J.; Nørskov, J. K. How copper catalyzes the electroreduction of carbon dioxide into hydrocarbon fuels. *Energy Environ. Sci.* **2010**, *3*, 1311–1315.
- (28) Cheng, J.; Sulpizi, M.; Sprik, M. Redox potentials and pK<sub>a</sub> for benzoquinone from density functional theory based molecular dynamics. *J. Chem. Phys.* **2009**, *131*, 154504.
- (29) Groß, A.; Sakong, S. Modelling the electric double layer at electrode/electrolyte interfaces. *Curr. Opin. Electrochem.* **2019**, *14*, 1–6.
- (30) Hansen, H. A.; Man, I. C.; Studt, F.; Abild-Pedersen, F.; Bligaard, T.; Rossmeisl, J. Electrochemical chlorine evolution at rutile oxide (110) surfaces. *Phys. Chem. Chem. Phys.* **2010**, *12*, 283–290.
- (31) Gossenberger, F.; Roman, T.; Groß, A. Equilibrium coverage of halides on metal electrodes. *Surf. Sci.* **2015**, *631*, 17–22.
- (32) Ringe, S.; Hörmann, N. G.; Oberhofer, H.; Reuter, K. Implicit Solvation Methods for Catalysis at Electrified Interfaces. *Chem. Rev.* **2022**, DOI: 10.1021/acs.chemrev.1c00675.
- (33) Huang, J.; Li, M.; Eslamibidgoli, M. J.; Eikerling, M.; Groß, A. Cation Overcrowding Effect on the Oxygen Evolution Reaction. *JACS Au* **2021**, *1*, 1752–1765.
- (34) Grimaud, A.; Diaz-Morales, O.; Han, B.; Hong, W. T.; Lee, Y.-L.; Giordano, L.; Stoerzinger, K. A.; Koper, M. T. M.; Shao-Horn, Y. Activating lattice oxygen redox reactions in metal oxides to catalyze oxygen evolution. *Nature Chem.* **2017**, *9*, 457–465.
- (35) Chen, X.; McCrum, I. T.; Schwarz, K. A.; Janik, M. J.; Koper, M. T. M. Co-adsorption of Cations as the Cause of the Apparent pH Dependence of Hydrogen Adsorption on a Stepped Platinum Single-Crystal Electrode. *Angew. Chem., Int. Ed.* **2017**, *56*, 15025–15029.
- (36) Ojha, K.; Doblhoff-Dier, K.; Koper, M. T. M. Double-layer structure of the Pt(111)-aqueous electrolyte interface. *Proc. Natl. Acad. Sci. U. S. A.* **2022**, *119*, No. e2116016119.
- (37) Jäckle, M.; Groß, A. Influence of electric fields on metal self-diffusion barriers and its consequences on dendrite growth in batteries. *J. Chem. Phys.* **2019**, *151*, 234707.
- (38) Roudgar, A.; Groß, A. Water bilayer on the Pd/Au(111) overlayer system: coadsorption and electric field effects. *Chem. Phys. Lett.* **2005**, *409*, 157.
- (39) Groß, A.; Gossenberger, F.; Lin, X.; Naderian, M.; Sakong, S.; Roman, T. Water Structures at Metal Electrodes Studied by Ab Initio Molecular Dynamics Simulations. *J. Electrochem. Soc.* **2014**, *161*, E3015–E3020.
- (40) Melander, M. M.; Kuisma, M. J.; Christensen, T. E. K.; Honkala, K. Grand-canonical approach to density functional theory of electrocatalytic systems: Thermodynamics of solid-liquid interfaces at constant ion and electrode potentials. *J. Chem. Phys.* **2019**, *150*, 041706.
- (41) Hörmann, N. G.; Andreussi, O.; Marzari, N. Grand canonical simulations of electrochemical interfaces in implicit solvation models. *J. Chem. Phys.* **2019**, *150*, 041730.
- (42) Hörmann, N. G.; Marzari, N.; Reuter, K. Electrosorption at metal surfaces from first principles. *npj Comput. Mater.* **2020**, *6*, 136.
- (43) Abidi, N.; Lim, K. R. G.; Seh, Z. W.; Steinmann, S. N. Atomistic modeling of electrocatalysis: Are we there yet? *Wiley Interdiscip. Rev. Comput. Mol. Sci.* **2020**, *11*, No. e1499.
- (44) Gossenberger, F.; Juarez, F.; Groß, A. Sulfate, Bisulfate, and Hydrogen Co-adsorption on Pt(111) and Au(111) in an Electrochemical Environment. *Front. Chem.* **2020**, *8*, 634.
- (45) Ooka, H.; Huang, J.; Exner, K. S. The Sabatier Principle in Electrocatalysis: Basics, Limitations, and Extensions. *Front. Energy Res.* **2021**, *9*, 654460.
- (46) Peng, Y.; Hajiyani, H.; Pentcheva, R. Influence of Fe and Ni Doping on the OER Performance at the Co<sub>3</sub>O<sub>4</sub>(001) Surface: Insights from DFT+U Calculations. *ACS Catal.* **2021**, *11*, 5601–5613.
- (47) Bhattacharyya, K.; Poidevin, C.; Auer, A. A. Structure and Reactivity of IrO<sub>x</sub> Nanoparticles for the Oxygen Evolution Reaction in Electrocatalysis: An Electronic Structure Theory Study. *J. Phys. Chem. C* **2021**, *125*, 4379–4390.
- (48) Chen, Z.; Cai, C.; Wang, T. Identification of Copper as an Ideal Catalyst for Electrochemical Alkyne Semi-hydrogenation. *J. Phys. Chem. C* **2022**, *126*, 3037–3042.
- (49) Juarez, F.; Yin, H.; Groß, A. Composition and Electronic Structure of Mn<sub>3</sub>O<sub>4</sub> and Co<sub>3</sub>O<sub>4</sub> Cathodes in Zinc–Air Batteries: A DFT Study. *J. Phys. Chem. C* **2022**, *126*, 2561–2572.
- (50) Fang, Y.; Ding, S.-Y.; Zhang, M.; Steinmann, S. N.; Hu, R.; Mao, B.-W.; Feliu, J. M.; Tian, Z.-Q. Revisiting the Atomistic Structures at the Interface of Au(111) Electrode–Sulfuric Acid Solution. *J. Am. Chem. Soc.* **2020**, *142*, 9439–9446.
- (51) Funtikov, A.; Linke, U.; Stimming, U.; Vogel, R. An in-situ STM study of anion adsorption on Pt(111) from sulfuric acid solutions. *Surf. Sci.* **1995**, *324*, L343–L348.
- (52) Sato, K.; Yoshimoto, S.; Inukai, J.; Itaya, K. Effect of sulfuric acid concentration on the structure of sulfate adlayer on Au(111) electrode. *Electrochem. Commun.* **2006**, *8*, 725–730.
- (53) Mathew, K.; Sundararaman, R.; Letchworth-Weaver, K.; Arias, T. A.; Hennig, R. G. Implicit solvation model for density-functional study of nanocrystal surfaces and reaction pathways. *J. Chem. Phys.* **2014**, *140*, 084106.
- (54) Sakong, S.; Groß, A. Water structures on a Pt(111) electrode from ab initio molecular dynamic simulations for a variety of electrochemical conditions. *Phys. Chem. Chem. Phys.* **2020**, *22*, 10431–10437.
- (55) Li, X.-Y.; Chen, A.; Yang, X.-H.; Zhu, J.-X.; Le, J.-B.; Cheng, J. Linear Correlation between Water Adsorption Energies and Volta Potential Differences for Metal/water Interfaces. *J. Phys. Chem. Lett.* **2021**, *12*, 7299–7304.
- (56) Le, J.-B.; Chen, A.; Li, L.; Xiong, J.-F.; Lan, J.; Liu, Y.-P.; Iannuzzi, M.; Cheng, J. Modeling Electrified Pt(111)-H<sub>2</sub>O/Water Interfaces from Ab Initio Molecular Dynamics. *JACS Au* **2021**, *1*, 569–577.
- (57) Mikkelsen, A. E. G.; Kristoffersen, H. H.; Schiøtz, J.; Vegge, T.; Hansen, H. A.; Jacobsen, K. W. Structure and energetics of liquid water–hydroxyl layers on Pt(111). *Phys. Chem. Chem. Phys.* **2022**, *24*, 9885–9890.
- (58) Heenen, H. H.; Gauthier, J. A.; Kristoffersen, H. H.; Ludwig, T.; Chan, K. Solvation at Metal/Water Interfaces: An ab initio Molecular Dynamics Benchmark of Common Computational Approaches. *J. Chem. Phys.* **2020**, *152*, 144703.
- (59) Garcia-Araez, N.; Climent, V.; Rodriguez, P.; Feliu, J. M. Elucidation of the Chemical Nature of Adsorbed Species for Pt(111) in H<sub>2</sub>SO<sub>4</sub> Solutions by Thermodynamic Analysis. *Langmuir* **2010**, *26*, 12408–12417.